Effect of Pretransitional Organization in Chiral Nematic of Oligothiophene Derivatives on Their Carrier Transport Characteristics

Masahiro Funahashi* and Nobuyuki Tamaoki*

Molecular Smart System Group, Nanotechnology Research Institute, National Institute of Advanced Industrial Science and Technology, Tsukuba Central 5-2, Higashi 1-1-1, Tsukuba, Ibaraki 305-8565, Japan

Received September 8, 2006. Revised Manuscript Received November 13, 2006

We have synthesized three phenylquaterthiophene derivatives (liquid-crystalline semiconductors that exhibit a chiral nematic phase) and investigated their carrier transport characteristics in the chiral nematic phases with the time-of-flight technique. In contrast to the ionic nature of negative carrier transport, positive carrier transport in the chiral nematic phases of these compounds should be attributed to electronic charge carrier transport. The temperature dependence of the positive carriers in the chiral nematic phases of these compounds were strongly affected by a pretransitional smectic order formation.

Introduction

In order to construct organic molecular systems with electronic and photonic functionalities, it is desirable to introduce a periodic structure into organic semiconductors by means of supramolecular self-assemblies because of the limitations of the microscopic processing of organic semiconductors. Chiral nematic liquid crystals are promising optical materials for reflective displays[1] and imaging devices[2] because the periodicities of their helical structures are of the order of the wavelengths in visible light. Circularly polarized photoluminescence[3] and laser emission from chiral nematic liquid crystals have been investigated recently;[4−7] however, only optical pumping was possible in these studies in which fluorescent dyes were doped in the cholesteric matrixes. The realization of electrical pumping systems, which are more practical, requires the construction of semiconductive cholesteric systems.

Electronic charge carrier transport has been confirmed in smectic systems[8−13] and discotic columnar phases[14−17] in which intermolecular packing structures promote intermolecular electronic charge transfer. In these phases, the temperature and electric field dependence of the electronic charge carrier mobility is small above room temperature because the intermolecular stacking structure in the smectic and columnar phases increases the intermolecular transfer integral and decreases the charge carrier hopping barrier as well as the distribution of energetic and spatial disorder. The glassy chiral nematic phase of a fluorene derivative exhibits good hole transporting properties, with mobility of the order of 10^{-4} cm^2/Vs,[18] in addition to the circularly polarized luminescence The carrier transport characteristics in the glassy nematic phase have been analyzed based on a correlation disorder model and the results were similar to the conventional organic amorphous semiconductors.[18] In contrast, only ionic carrier transport has been observed in fluidic nematic and chiral nematic phases because ionic impurities or ionized liquid crystal molecules easily move in media with low viscosity and intermolecular electronic charge hopping is low due to a low transfer integral.[19−23]

Recently, electronic charge carrier transport has been confirmed in the fluidic chiral nematic phase of a phenylquaterthiophene derivative[24] and the nematic phase of dialkyl-

* Corresponding author. E-mail: Masahiro-funahashi@aist.go.jp, n.tamaoki@aist.go.jp.

(1) Yang, D. K.; Chien, L. C.; Doane, J. W. *IDRC, Proc.* **1991**, 49.
(2) Tamaoki, N.; Parfenov, A. V.; Masaki, A.; Matsuda, H. *Adv. Mater.* **1997**, *9*, 1102.
(3) Woon, K. L.; O'Neill, M.; Richards, G. J.; Aldred, M. P.; Kelly, S. M.; Fox, A. M. *Adv. Mater.* **2003**, *15*, 1555.
(4) Finkelmann, H.; Kim, S. T.; Munoz, A.; Palffy-Muhoray, P.; Taheri, B. *Adv. Mater.* **2001**, *13*, 1069.
(5) Furumi, S.; Yokoyama, S.; Otomo, A.; Mashiko, S. *Appl. Phys. Lett.* **2004**, *84*, 2491.
(6) Araoka, F.; Shin, K.; Takanishi, Y.; Ishikawa, K.; Takezoe, H.; Zhu, Z; Swager, T. M. *J. Appl. Phys.* **2003**, *94*, 279.
(7) Ozaki, M.; Kasano, M.; Ganzke, D.; Haase, W.; Yoshino, K. *Adv. Mater.* **2002**, *14*, 306.
(8) Funahashi, M.; Hanna, J. *Phys. Rev. Lett.* **1997**, *78*, 2184.
(9) Funahashi, M.; Hanna, J. *Appl. Phys. Lett.* **1997**, *71*, 602.
(10) Funahashi, M.; Hanna, J. *Appl. Phys. Lett.* **2000**, *76*, 2574.
(11) Funahashi, M.; Hanna, J. *Mol. Cryst. Liq. Cryst.* **2004**, *410*, 529.
(12) Funahashi, M.; Hanna, J. *Adv. Mater.* **2005**, *17*, 594.
(13) Funahashi, M.; Hanna, J. *Mol. Cryst. Liq. Cryst.* **2001**, *368*, 4078.
(14) Adam, D.; Closs, F.; Frey, T.; Funhoff, D.; Haarer, D.; Ringsdorf, H.; Schuhmacher, P.; Siemensmeyer, K. *Phys. Rev. Lett.* **1993**, *70*, 457.
(15) Adam, D.; Schuhmacher, P.; Simmerer, J.; Häussling, L. H.; Paulus, W.; Siemensmeyer, K.; Etzbach, K. H.; Ringsdorf, H.; Haarer, D. *Adv. Mater.* **1995**, *7*, 276.
(16) van de Craats, A. M.; Warman, J. M.; Müllen, K.; Geerts, Y.; Brand, J. D. *Adv. Mater.* **1998**, *10*, 36.
(17) Pecchia, A.; Lozman, O. R.; Movaghar, B.; Boden, N.; Bushby, R. *Phys. Rev. B* **2002**, *65*, 1064204.
(18) Farrar, S. R.; Contoret, A. E. A.; O'Neill, M.; Nicholls, J. E.; Richards, G. J.; Kelly, S. M. *Phys. Rev. B* **2002**, *66*, 125107
(19) Shimizu, Y.; Shigeta, K.; Kusabayashi, S. *Mol. Cryst. Liq. Cryst.* **1986**, *140*, 105.
(20) Yoshino, K.; Tanaka, N.; Inuishi, Y. *Jpn. J. Appl. Phys.* **1976**, *15*, 735.
(21) Murakami, S.; Naito, H.; Okuda, M.; Sugiyama, A. *J. Appl. Phys.* **1995**, *78*, 4533.
(22) Sawada, A.; Manabe, A.; Naemura, S. *Jpn. J. Appl. Phys.* **2001**, *40*, 220.
(23) Sawada, A.; Naemura, S. *Jpn. J. Appl. Phys.* **2002**, *41*, L195.
(24) Funahashi, M.; Tamaoki, N. *Chemphyschem.* **2006**, *7*, 1193.

10.1021/cm0621287 CCC: $37.00
Published on Web 01/10/2007

fluorene derivatives as well as glassy nematic compounds.[25] The liquid-crystal materials reported in these papers are characterized as large extended π-conjugated systems that enhance the intermolecular hopping of charge carriers due to a large intermolecular transfer integral. We reported that carrier mobility in the chiral nematic phase saturated with an increase in the temperature; this is different from the case of ionic transport in which the ionic mobility monotonically increases with the temperature. The saturation in the electronic charge carrier transport could be caused by the competition between the thermal activation of charge carrier hopping and the thermal disorder; however, no direct evidence has been confirmed. M. O'Neill et al. reported high carrier mobility up to 10^{-3} cm^2/Vs in the nematic phase of fluorene derivatives with a large π-conjugated system.[25] The nematic phase of the fluorene derivatives with small π-conjugation exhibits low carrier mobility with a positive temperature dependence, while the phases with large π-conjugated systems exhibit high carrier mobility up to 10^{-3} cm^2/Vs with a complicated temperature dependence whose origin is not clear at present. The temperature dependences of the carrier mobility in the nematic and chiral nematic phases are quite different from those in the smectic phases in which the carrier mobility is almost independent of the temperature.

In this paper, we compare the carrier transport in the chiral nematic phases of some phenylquaterthiophene derivatives and clarify the temperature dependence of the carrier mobility. In addition, we also discuss the influence of microscopic pretransitional organization in the chiral nematic phases on the carrier transport characteristics, which are reflected in the cybotactic peak in the low-angle region in the X-ray diffraction image.

Materials and Methods

Synthesis of Phenylquaterthiophene Derivatives. Oligothiophene derivatives such as sexithiophene are typical organic semiconductors that have been employed in thin-film transistors.[26−31] ω,ω'-Dialkyloligothiophene[10,32] and ω,ω'-alkylalkynyloligothiophene,[12] which exhibit smectic phases, have also been investigated, and high carrier mobilities were reported in the highly ordered smectic phases because of an extended π-orbital that includes sulfur atoms with a large van der Waals radius.

In this study, oligothiophene derivatives that exhibit the chiral nematic phase were designed. In order to enhance the intermolecular hopping of charge carriers, an extended π-conjugated system is effective. On the other hand, crystallization was inhibited by the laterally substituted methyl group. Three phenylquaterthiophene derivatives with different alkyl chain lengths and different positions of the methyl substitutent were synthesized as shown in Figure 1. 2-Alkylquaterthiophene skeletons were constructed by sequential Ni(0)-catalyzed coupling reactions with thenylmagnesium bromide according to the literature.[33] After the iodination of the 5′′′′ position of the 2-alkylquaterthiophene derivatives, the three 2-alkyl-5′′′′-phenylquaterthiophene derivatives were synthesized by a Pd(0)-catalyzed Suzuki coupling reaction[34] between the bromide and 4-((*S*)-2-methylbutyloxyphenyl)boric acid 2,2-dimethylpropanediyl ester. 2-Bromo-5-alkylthiophenes were commercially available and used without purification.

5-Iodo-3-methyl-2′′′-propyl-2:5′-2′:5′′-2′′:5′′′-quarterthiophene (2). To a THF solution (100 mL) of 3-methyl-2′′′-propyl-2:5′-2′:5′′-2′′:5′′′-quarterthiophene (**1**) (2.00 g, 0.00518 mol) was added Bu^{n}Li hexane solution (1.6 M, 5.5 mL, 0.0088 mol) at 0 °C. After stirring for 30 min, iodine (2.00 g, 0.0079 mol) was added to the solution that was cooled to −78 °C. After stirring for 1 h at room temperature, diluted hydrochloric acid was added to the reaction mixture. It was extracted with THF and dried over Na_2SO_4. After the evaporation of the solvent, a yellow solid was obtained. The crude product was recrystallized from n-hexane, and yellow powder crystals (1.84 g, 69.4%) were obtained. ^{1}H NMR δ (ppm, $CDCl_3$) = 1.00 (3H, t, J = 7.4 Hz), 1.71 (2H, sextet, J = 7.4 Hz), 2.37 (3H, s), 2.78 (2H, t, J = 7.4 Hz), 6.69 (1H, d, J = 3.6 Hz), 6.97 (1H, d, J = 4.1 Hz), 6.99 (1H, d, J = 4.1 Hz), 7.00 (1H, d, J = 3.6 Hz), 7.03 (1H, s), 7.06 (1H, d, J = 3.8 Hz), 7.09 (1H, d, J = 3.8 Hz). IR (KBr disk) 463.79, 802.30, 828.28, 844.67, 1446.35, 1456.96, 1505.17, 2335.38, 2362.38, 2858.00, 2868.61, 2921.64, 2952.50, 3062.42 cm^{-1}. Mass (ESI) Found: *m*/*e*: 512.37, 513.38, 514.38, 515.38, 516.38. Calculated: *m*/*e*: 511.93, 512.93, 513.92, 514.92. Anal. Found: C, 47.15; H, 3.28; S, 24.91. Calculated: C, 46.87; H, 3.34; S, 25.03.

5-Iodo-3′′-methyl-2′′′-propyl-2:5′-2′:5′′-2′′:5′′′-quarterthiophene (5). This compound was synthesized from **4** in a manner identical to that of 5-iodo-3-methyl-2′′′-propyl-2:5′-2′:5′′-2′′:5′′′-quarterthiophene (**2**). The yield was 50%. ^{1}H NMR δ (ppm, $CDCl_3$) = 1.00 (3H, t, J = 7.4 Hz), 1.73 (2H, sext, J = 7.4 Hz), 2.36 (3H, s), 2.80 (2H, t, J = 7.4 Hz), 6.74 (1H, d, J = 3.6 Hz), 6.83 (1H, d, J = 3.8 Hz), 6.95 (1H, s), 6.96 (1H, d, J = 4.9 Hz), 7.00 (1H, d, J = 3.8 Hz), 7.02 (1H, d, J = 3.8 Hz), 7.16 (1H, d, J = 3.6 Hz). IR (KBr disk) 418.5, 460.9, 791.7, 838.9, 1212.0, 1416.5, 1456.9, 1501.3, 2859.9, 2924.5, 2949.6 cm^{-1}. Mass (ESI) Found: *m*/*e*: 512.29, 513.29, 514.28, 515.28. Calculated: *m*/*e*: 511.93, 512.93, 513.92, 514.92. Anal. Found: C,47.23; H, 3.25; S, 25.16. Calculated: C,46.87; H, 3.34; S, 25.03.

5-Iodo-3-methyl-2′′′-dodecyl-2:5′-2′:5′′-2′′:5′′′-quarterthiophene (8). This compound was synthesized from **7** in a manner identical to that of 5-iodo-3-methyl-2′′′-propyl-2:5′-2′:5′′-2′′:5′′′-quarterthiophene (**2**). The yield was 52%. ^{1}H NMR δ (ppm, $CDCl_3$) = 0.88 (3H, t, J = 7.5 Hz), 1.20−1.52 (18H, m), 1.69 (2H, sextet, J = 7.5 Hz), 2.36 (3H, s), 2.81 (2H, t, J = 7.5 Hz), 6.73 (1H, d, J = 3.6 Hz), 6.83 (1H, d, J = 3.7 Hz), 6.94 (1H, s), 6.95 (1H, d, J = 3.7 Hz), 7.00 (1H, d, 3.8 Hz), 7.02 (1H, d, J = 3.8 Hz), 7.15 (1H, d, J = 3.6 Hz). IR (KBr disk) 417.5, 459.9, 720.3, 828.3, 839.8, 1416.5, 1436.7, 1463.7, 1502.3, 2845.8, 2908.3, 2922.6, 2948.6 cm^{-1}. Mass (ESI) Found: m/e: 638.51, 639.51, 640.51, 641.51. Calculated: m/e: 638.07, 639.07, 640.06, 641.07. Anal. Found: C, 54.80; H, 5.50; S, 20.14. Calculated: C, 54.53; H, 5.52; S, 20.08.

5-(4-[(*S*)-2-Methylbutoxy]phenyl)-3-methyl-2′′′-propyl-2:5′-2′:5′′-2′′:5′′′-qua rterthiophene (3-QTP4MePh-O5*) (3). 5-Iodo-3-methyl-2′′′-propyl-2:5′-2′:5′′-2′′:5′′′-quarterthiophene (**2**) (0.63 g,

(25) Woon, K. L.; Aldred, M. P.; Vlachos, P.; Mehl, G. H.; Stirner, T.; Kelly, S. M.; O'Neill, M. *Chem. Mater.* **2006**, *18*, 2311.
(26) Hajlaoui, R.; Horowitz, G.; Garnier, F.; Arce-Bronchet, A.; Laigyre, L.; Kassmi, A. E.; Damanze, F.; Konki, F. *Adv. Mater.* **1997**, *9*, 389.
(27) Dodabalapur, A.; Katz, H. E.; Tosi, L.; Haddon, R. C. *Science* **1995**, *269*, 1560.
(28) Horowitz, G.; Hajlaoui, M. E.; Hajlaoui, R. *J. Appl. Phys.* **2000**, *87*, 4456.
(29) Halik, M.; Klauk, H.; Zschieschang, U.; Schmid, G.; Radlik, W.; Ponomarenko, S.; Kirchmeyer, S.; Weber, W. *J. Appl. Phys.* **2003**, *93*, 2977.
(30) Garnier, F.; Hajlaoui, R.; Kassmi, A. E.; Horowitz, G.; Laiyre, L.; Porzio, W.; Armanini, A.; Provasoli, F. *Chem. Mater.* **1998**, *10*, 3334.
(31) Ponomarenko, S.; Kirchmeyer, S. *J. Mater. Chem.* **2003**, *13*, 197.
(32) Azumi, R.; Götz, G.; Bäuerle, P. *Synth. Met.* **1999**, *101*, 569.
(33) Geng, Y.; Fechtenköttner, A.; Müllen, K. *J. Mater. Chem.* **2001**, *11*, 1634.
(34) Miyaura, N.; Yanagi, T.; Suzuki, A. *Synth. Commun.* **1981**, *11*, 513.

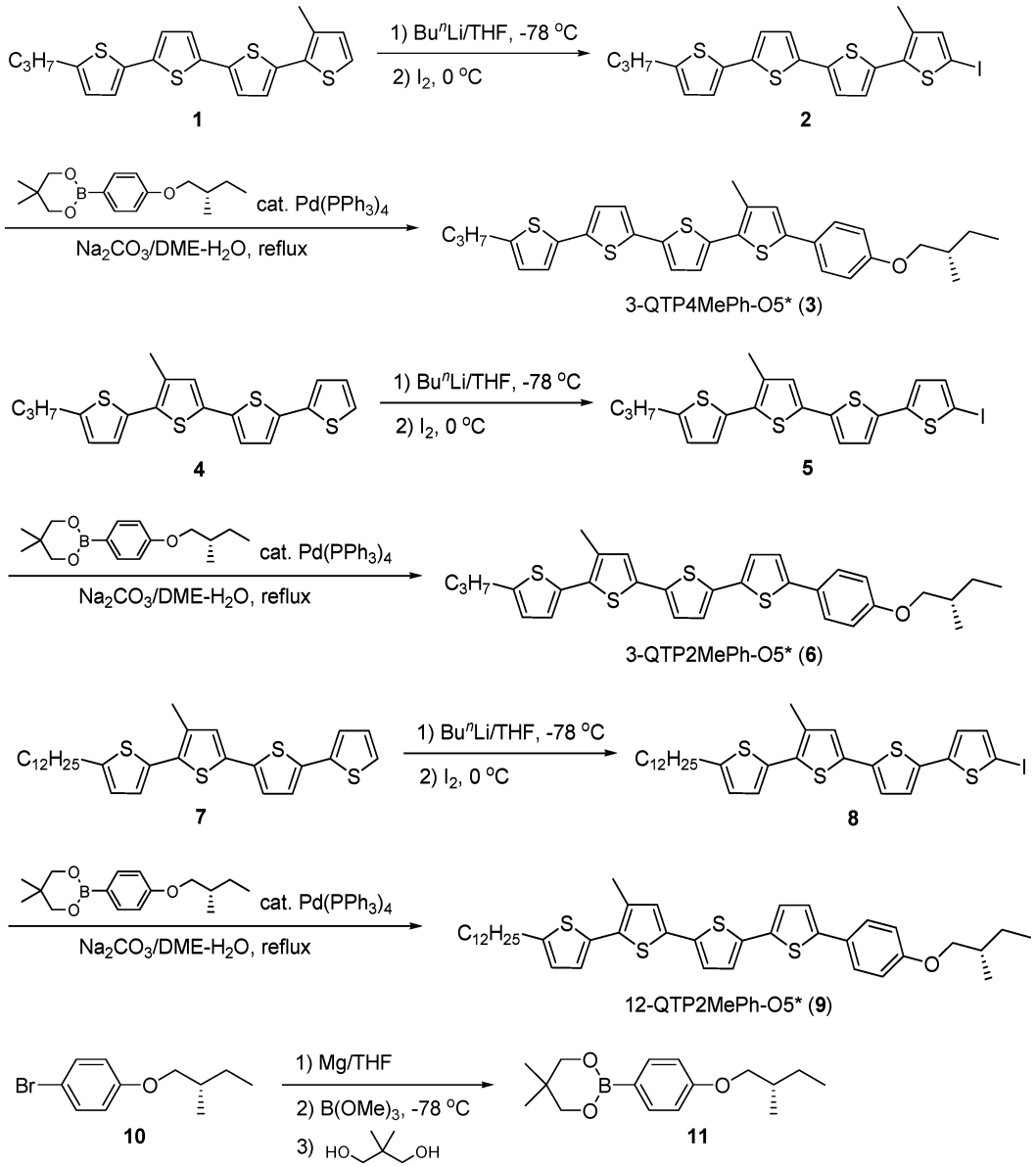

Figure 1. Synthetic route of the oligothiophene derivatives exhibiting a chiral nematic phase.

1.23 mmol), 4-[(*S*)-2-methyl-butoxy]-phenyl boric acid 2,2-dimethylpropanediyl ester (**11**) (0.53 g, 2.2 mol), and tetrakis-(triphenylphophine)palladium(0) (53.5 mg, 0.046 mmol) were dissolved in dimethoxyethene (100 mL), and 10 wt % of an aqueous solution of Na_2CO_3 was added to the reaction solution. The reaction mixture was refluxed at 120 °C for 1 h. After cooling to room temperature, water was added to the reaction solution. Yellow crystals were obtained by filtering. The crude product was purified with column chromatography (silica gel, the elutant was hot cyclohexane). The purified product was recrystallized from n-hexane and orange needle crystals (0.58. g, 86%) were obtained. ^{1}H NMR δ (ppm, $CDCl_3$) = 0.96 (3H, t, J = 7.4 Hz), 1.00 (3H, t, J = 7.4 Hz), 1.02 (3H, d, J = 6.8 Hz), 1.27 (1H, sextet, J = 6.3 Hz), 1.58 (1H, sextet, J = 6.0 Hz), 1.69 (2H, sextet, J = 7.4 Hz),1.87 (1H, octet, J = 6.6 Hz), 2.42 (3H, s), 2.78 (2H, t, J = 7.4 Hz), 3.76 (1H, dd, J = 6.6 Hz, 9.0 Hz), 3.85 (1H, dd, J = 6.0 Hz, 9.0 Hz), 6.69 (1H, d = J = 3.6 Hz), 6.90 (2H, d, J = 8.7 Hz), 6.99 (1H, d, J = 4.2 Hz), 7.00 (1H, s), 7.00 (1H, d = J = 3.9 Hz), 7.04 (1H, d, J = 3.6 Hz), 7.06 (1H, d, J = 3.6 Hz), 7.11 (1H, d, J = 3.9 Hz), 7.49 (2H, d, J = 8.7 Hz). ^{13}C NMR δ (ppm, $CDCl_3$) = 27.45, 29.79, 31.94, 32.65, 40.93, 42.26, 48.35, 50.84, 89.11, 92.71, 93.14, 93.56, 131.02, 139.50, 139.72, 139.91, 140.15, 141.09, 141.68, 142.56, 142.60, 142.88, 145.40, 150.66, 151.06, 151.42, 151.89, 152.45, 152.90, 157.82, 161.47, 175.21. IR (KBr disk) 789.7, 822.5, 1037.5, 1181.2, 1247.7, 1447.3, 1460.8, 1502.3, 2870.5, 2948.7, 2956.4 cm^{-1}. Mass (ESI) Found: *m*/*e*: 548.1 (100%), 549.1 (66%), 550.1 (31%) Calculated: *m*/*e*: 548.13 (100%), 549.14 (34%), 550.13 (18%). Anal. Found: C, 67.74; H, 5.86; O, 2.80; S, 23.25. Calculated: C, 67.84; H, 5.88; O, 2.92; S, 23.37.

5-(4-[(*S*)-2-Methylbutoxy]phenyl)-3″-methyl-2‴-propyl-2:5′-2′:5″-2″:5‴-quarterthiophene (3-QTP2MePh-O5*) (6). This compound was synthesized from **5** and **11** in a manner identical to that of 5-(4-[(*S*)-2-methylbutoxy]phenyl)-3-methyl-2‴-propyl-2:5′-2′:5″-2″:5‴-quarterthi ophene (3-QTP4MePh-O5*) (**3**). Yellow needle crystals were obtained (92%). ^{1}H NMR δ (ppm, $CDCl_3$) = 0.96 (3H, t, J = 7.5 Hz), 1.01 (3H, t, J = 7.2 Hz), 1.03 (3H, d, J = 6.1 Hz), 1.28 (1H, sextet, J = 7.5 Hz), 1.58 (1H, septet, J = 5.7 Hz), 1.73 (2H, sextet, J = 7.5 Hz), 1.88 (1H, sextet, J = 6.1 Hz), 2.37 (3H, s), 2.80 (2H, t, J = 7.5 Hz), 3.76 (1H, dd, J = 6.6 Hz, 9.0 Hz), 3.85 (1H, dd, J = 6.0 Hz, 9.0 Hz), 6.74 (1H, d, J = 3.6 Hz), 6.91 (2H, d, J = 8.7 Hz), 6.95 (1H, s), 6.96 (1H, d, J = 4.1 Hz), 7.04 (1H, d, J = 3.8 Hz), 7.06 (1H, d, J = 3.8 Hz), 7.10 (2H, s), 7.51 (2H, d, J = 8.7 Hz). ^{13}C NMR δ (ppm, $CDCl_3$) = 11.40, 13.80, 15.60, 16.61, 24.91, 26.21, 32.25, 34.78, 73.08, 115.02,

122.72, 124.02, 124.09, 124.56, 124.69, 125.19, 126.16, 126.94, 127.84, 133.82, 134.01, 134.35, 134.68, 135.46, 135.48, 135.83, 136.29, 145.94, 159.21. IR (KBr disk) 476.3, 791.7, 826.4, 841.8, 1018.2, 1176.4, 1247.7, 1459.9, 1500.4, 2838.7, 2872.6, 2931.3, 2954.4 cm^{-1}. Mass (ESI) Found: *m*/*e*: 548.1 (100%), 549.1 (66%), 550.1 (31%). Calculated: *m*/*e*: 548.13 (100%), 549.14 (34%), 550.13 (18%). Anal. Found: C, 68.18; H, 5.92; O, 2.80; S, 23.35. Calculated: C, 67.84; H, 5.88; O, 2.92; S, 23.37.

5-(4-[(*S*)-2-Methylbutoxy]phenyl)-3‴-methyl-2‴-dodecyl-2:5′-2′:5″-2″:5‴-quarterthiophene (12-QTP2MePh-O5*) (9). This compound was synthesized from **8** and **11** in a manner identical to that of 5-(4-[(*S*)-2-methylbutoxy]phenyl)-3-methyl-2‴-propyl-2:5′-2′:5″-2″:5‴-quarterthiophene (3-QTP4MePh-O5*) (**3**). Yellow solids were obtained (67%). ^{1}H NMR δ (ppm, $CDCl_3$) = 0.88 (3H, t, J = 6.9 Hz), 0.96 (3H, t, J = 7.5 Hz), 1.02 (3H, d J = 6.6 Hz), 1.20−1.42 (19H, m), 1.58 (1H, sextet, J = 5.9 Hz), 1.70 (2H, sextet, J = 6.9 Hz), 1.88 (1H, octet, J = 6.7 Hz), 2.36 (3H, s), 2.81 (2H, t, J = 7.5 Hz), 3.76 (1H, dd, J = 6.6 Hz, 9.0 Hz), 3.85 (1H, dd, J = 6.0 Hz, 9.0 Hz), 6.73 (1H, d = J = 3.6 Hz), 6.91 (2H, d, J = 8.7 Hz), 6.95 (1H, s), 6.95 (1H, d, J = 3.3 Hz), 7.03 (1H, d, J = 3.8 Hz), 7.06 (1H, d, J = 3.8 Hz), 7.10 (2H, s), 7.51 (2H, d, J = 8.7 Hz). ^{13}C NMR δ (ppm, $CDCl_3$) = 11.39, 14.20, 15.60, 16.00, 16.61, 22.77, 26.21, 29.21, 29.43, 29.63, 29.72, 29.74, 30.02, 30.22, 31.69, 32.00, 34.79, 73.10, 115.02, 122.71, 124.01, 124.08, 124.56, 125.18, 126.60, 126.94, 127.84, 130.89, 133.72, 133.81, 133.99, 135.39, 135.84, 136.28, 143.48, 146.25, 159.21. IR (KBr disk) 471.5, 788.9, 824.4, 1175.4, 1250.6, 1284.4, 1462.7, 1499.4, 2847.4, 2869.6, 2913.9, 2956.4 cm^{-1}. Mass (MALDI-TOF) Found: *m*/*e*: 674.04, 675.05, 676.3, 677.06. Calculated: *m*/*e*: 674.27, 675.28, 676.27, 677.27. Anal. Found: C, 67.74; H, 5.86; O, 2.80; S, 23.2. Calculated: C, 67.84; H, 5.88; O, 2.92; S, 23.37.

Characterization of Mesophases of the Phenylquaterthiophene Derivatives. The phase-transition temperature and transition enthalpy were determined by differential scanning calorimetry (DSC, Seiko DSC-6200). Phase identification was carried out by the observation of the optical texture of the mesophases under a polarized light microscope (Olympas BH-2) equipped with a hot stage (Mettler FP90) and X-ray diffraction (Rigaku RINT-2000); in this experiment, the X-ray (Cu Kα_1) was transmitted through a quartz tube filled with a liquid-crystal sample, and the diffraction pattern was recorded on a 2D imaging plate. In this study, the liquid-crystal sample was not aligned, and the $\theta-2\theta$ curve was obtained by integration of the 2D diffraction image around the center of the plate.

Viscosity Measurement. The temperature-dependence of the macroscopic viscosity determined by a capillary viscometer can be a measure to *judge* whether the carrier transport mechanism is electronic or ionic although it is difficult to determine all the viscosity tensor components considering its anisotropy.[21−23] The viscosity in the isotropic and chiral nematic phases was measured with glass capillaries placed on a hot stage. The relative viscosity was calculated from the time interval during which the sample flowed through the capillary tube.[21] In this method, the viscosity of the isotropic and chiral nematic phases could be measured while that of the chiral smectic phase could not be determined because of its very high magnitude.

In the three compounds, the viscosity increased monotonically with the temperature and continuously changed at the phase transition from the chiral nematic to the isotropic phase. In the chiral nematic phase of the compounds, the temperature dependence of the viscosity was of the Arrhenius type in which the activation energy was 0.3 eV in 3-QTP4MePh-O5*, 0.6 eV in 3-QTP-2MePh-O5*, and 0.5 eV in 12-QTP2MePh-O5*.

Time-of-Flight Measurement Setup. The carrier mobility was determined by the conventional time-of-flight technique;[36] the apparatus consisted of a pulse laser (THG of a Nd:YAG laser (Laser Photonics; wavelength, 355 nm; pulse duration, 1 ns)) for excitation, the sample on a hot stage, a serial resistor, and a digital oscilloscope (Tektronics MD-600B). All measurements were carried out under atmospheric conditions. An electric field was applied to the liquid-crystal cell consisting of two ITO-coated glass plates. The pulse laser illuminated one side of the cell. When the absorption coefficient of a sample is sufficiently large, the excitation pulse is absorbed and a sheet of photocarriers is generated near the illuminated electrode. In this study, the neat film of the three compounds exhibited a strong absorption band around 400 and 250 nm in the chiral nematic phase; the depth of penetration of the excitation light at 356 nm was estimated to be less than 0.5 μm, i.e., it was much smaller than the sample thickness. Under the influence of the electric field, the photogenerated carriers drifted across the bulk of the sample, inducing a displacement current through the serial resistor. When the charge carriers arrived at the counter electrode, the induced displacement current decreased to zero. Therefore, the kink point in the transient photocurrent curve corresponds to the transit time t_T. Using eq 1, the carrier mobility (μ) can be calculated from the values of t_T, the sample thickness d, and the applied voltage V:

$$\mu = \frac{d^2}{Vt_T} \tag{1}$$

Illuminating the electrode under a positive or negative bias allows the positive or negative carrier mobility to be determined, respectively.

For the observation of optical textures under the application of an electric field using a polarized light microscope, we prepared liquid-crystal cells (thicknesses: 4 and 9 μm) on two ITO-coated glass plates. In the absence of an electric field, we observed a Granjan texture, which was characteristic of a chiral nematic phase, in the chiral nematic phase of the three compounds; this indicated the planar alignment of the liquid-crystal molecules. After applying an electric field (applied voltage > 10 V) to the 9-μm-thick sample, we observed a fingerprint texture that indicated that the helical axis was parallel to the electrode surface. From the periodicity of the observed fingerprint texture, the helical pitch was ca. 7 μm for 3-QTP4MePh-O5*, i.e., it was comparable to the thickness of the sample (9 μm). The helical pitches in the chiral nematic phases of 3-QTP2MePh-O5* and 12-QTP2MePh-O5* were of the same order. The helical twisting power of the compounds should not be so large as to induce a helical structure having a short periodicity. These oligothiophene derivatives have a small permanent dipole moment perpendicular to the molecular axis as well as an induced dipole moment along the axis because of the long π-conjugated system. Under a strong electric field, the induced dipole exceeds the permanent dipole, thus causing a change in the molecular alignment. Therefore, we observed a change of the direction of the helical axis from perpendicular to parallel with regard to the surface when the electric field was applied. We performed the electrical measurements in an alignment where the helical axis was parallel to the electrode surface; with this alignment, some molecules were perpendicular to the surface, while other molecules were parallel to the surface. If the anisotropy in the carrier mobility is large in this phase, some carriers can drift faster than others. The transient photocurrent was obtained by integration of the photocurrent caused

(35) Collings, J. *Liquid Crystals − Nature's delicate phase of matter*; Princeton University Press: New Jersey, 1990
(36) Kepler, R. G. *Phys. Rev.* **1960**, *119*, 1226.

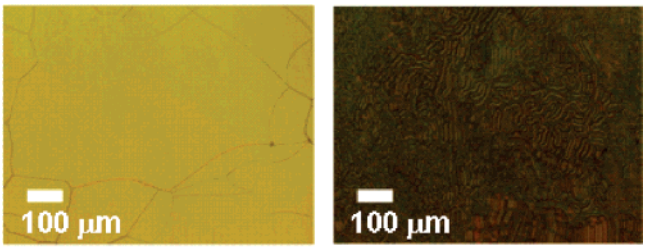

Figure 2. Micrographic texture in the chiral nematic phase of 3-QTP4MePh-O5* at 120 °C under a polarized light microscope: (a) without an electric field and (b) under an electric field (30 V). The liquid-crystal cell consisted of two ITO-coated glass plates with a thickness of 9 μm.

by carriers with various drift velocities and therefore the dispersion of carriers should be larger, exhibiting a slow current decay or a long tail in the transient photocurrent curves. However, the obtained transient photocurrent decay was sharp and no current tailing appeared. The dispersion and anisotropy in the phase should not be very large.

Results and Discussion

In the chiral nematic phases of the three compounds, nondispersive transients were obtained for positive and negative carriers, and the carrier mobilities could be determined clearly overall mesomorphic temperature ranges and a wide range of the electric field between 10^5 and 10^4 V/cm. The negative carrier mobilities were of the order of 10^{-5} cm^2/Vs at 150 °C, and the temperature dependences of the compounds were of the Arrhenius type. The negative carrier mobility in the chiral nematic phase of the three compounds increased monotonically with the temperature. The positive carrier mobilities in the chiral nematic phases of these compounds were of the order of 10^{-4} cm^2/Vs above 150 °C. However, the temperature dependence of the positive carrier mobility was quite different among these three compounds. 3-QTP4MePh-O5* exhibited saturation in the positive carrier mobility with an increase in the temperature, which was in contrast to the behavior of 3-QTP2MePh-O5* where the positive carrier mobility was independent of temperature; in the chiral nematic phase of 12-QTP4MePh-O5*, the positive carrier mobility decreased with an increase in the temperature. These three compounds had almost the same aromatic core structure, which contributed to the carrier transport process; however, they had different alkyl chain and methyl group substitutions, which could influence the molecular self-organization.

Characterization of the Mesophase of the Phenylquaterthiophene Derivatives. 3-QTP4MePhO5* exhibited only the chiral nematic phase and crystallized at 87 °C while 3-QTP2MePh-O5* and 12-QTP2MePh-O5*, in which the 5′ position of the second thiophene ring was substituted by a methyl group, exhibited a chiral smectic C phase below the chiral nematic phase. In the observations obtained using the polarized light microscope, Granjan textures were observed in the chiral nematic phases of the three compounds without an electric field, as shown in Figure 2a; this indicated a planar molecular alignment of the surface of the substrates. Under the application of an electric field, fingerprint textures, which indicated that the helical axis was parallel to the electrode surface, were observed in the chiral nematic phases of these compounds, as shown in Figure 2b.[35] In the chiral nematic phases of these compounds, the helical pitch, which was determined from the fingerprint texture appearing under the application of an electric field, was of the order of several micrometers; this was much larger than the wavelength of visible light, resulting in the absence of interference colors in the visible region. The chiral smectic phases of 3-QTP2-MePh-O5* and 12-QTP2MePh-O5* were confirmed by broken fan-like textures observed under a polarized light microscope as well as by the ferroelectric switching of the optical texture under the application of an electric field, which will be reported elsewhere. 12-QTP2MePh-O5* exhibited another smectic phase below the chiral smectic phase. The smectic phase had higher order than the chiral smectic phase from X-ray diffraction; however, the phase structure could not be identified.

Table 1

compound	phase transition temperature °C (transition enthalpy (J/g))
3-QTP4MePh-O5*	K 111 (53.8) N* 183 (1.5) Iso : heating Iso 184 (1.3) N* 86 (43.4) K : cooling
3-QTP2MePh-O5*	K 145 (48.7) N* 197 (1.4) Iso : heating Iso 197 (1.5) N* 143 (3.6) SmC* 137 (40.5) K : cooling
12-QTP2MePh-O5*	K 87 (7.2) SmX 112 (3.1) SmC* 146 (0.31) N* 166 (0.38) Iso : heating
Iso	165 (0.283) N* 144 (0.27) SmC* 110 (2.9) SmX 56 (7.3) K : cooling

[a] Iso, isotropic phase; N*, chiral nematic phase; SmC*, chiral smectic phase; K, crystal phase.

In the DSC measurement, small peaks (ΔH = 0.3−2 mJ/mg) corresponded to the transition from the isotropic to the chiral nematic phase in the three compounds both in heating and cooling processes. Below the small peak, a relatively large peak (ΔH = 3.6 mJ/mg) appeared in the case of 3-QTP-2Me-Ph-O5*, which corresponded to the transition from the chiral nematic to the monotropic SmC* phase. In 12-QTP-2Me-Ph-O5*, the transition enthalpy from the chiral nematic to the SmC* phase was very small; this was comparable to that from the isotropic to the chiral nematic phase. This small transition enthalpy should be associated with the pretransitional smectic order formation that will be discussed later. In addition, a transition from the SmC* to the highly ordered smectic phase was also observed. The phase transition temperature and transition enthalpy are summarized in Table 1.

In the X-ray diffraction of the chiral nematic phases of the three compounds, only a broad halo was observed in the wide-angle region, and a single sharp reflection was observed in the low-angle region in the chiral smectic phases of 3-QTP2MePh-O5* and 12-QTP2MePh-O5*. It should be noted that the cybotactic peak in the low-angle region was observed in the temperature region near the phase-transition point from the chiral nematic phase to the chiral smectic phase of 3-QTP2MePh-O5* and 12-QTP2MePh-O5*.

Carrier Transport in the Chiral Nematic Phase of 3-QTP4MePh-O5*. The carrier transport characteristics of 3-QTP4MePh-O5* have already been described in another paper.[24] The nondispersive transient photocurrent curves were obtained for positive carriers for the entire temperature range of the chiral nematic phase, which corresponded to a mobility of the order of 10^{-4} cm^2/Vs. For negative carriers, single transits at the longer time region than that of the positive

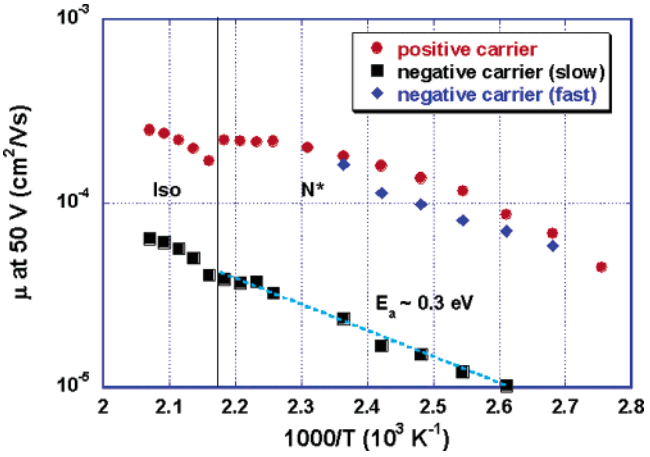

Figure 3. Ahrrenius plot of the carrier mobility in the chiral nematic and isotropic phases of 3-QTP4MePh-O5*.

carrier were observed in the high-temperature region, while two transits that corresponded to mobilities of the order of 10^{-4} and 10^{-5} cm^2/Vs were observed in the low-temperature region. As shown in Figure 3, below 130 °C, the positive carrier mobility increased with the temperature; however, it saturated *above* this temperature. This dependence was quite different from the temperature dependence of the viscosity, which increased monotonically with the temperature. Therefore, the positive carrier transport was identified to be electronic in nature. The negative carrier mobility at longer time region exhibited the Arrhenius type of temperature dependence with an activation energy of 0.4 eV, which was identical with that of the inverted viscosity. Therefore, the slower negative carrier transport was attributed to ionic transport. The faster negative carrier transport should be ascribed to an electronic process. However, a precise discussion was difficult because of the weak photocurrent signal.

It is speculated that the temperature dependence of the electronic carrier mobility should be determined by two factors: the thermal activation of charge carrier hopping, which causes a positive temperature dependence, and the dynamic disorder effect, which causes a negative temperature dependence of the carrier mobility. In the high-temperature region of the chiral nematic phase, the dynamic disorder effect should cancel out the positive temperature dependence caused by the thermally activated charge carrier hopping and result in saturation. In the isotropic phase, the positive carrier mobility again increased with the temperature; this should be attributed to the hopping of electronic charge carriers or ionic carrier transport that is thermally activated by the disappearance of the molecular assembling structure.

Carrier Transport in the Chiral Nematic Phase of 3-QTP2MePh-O5*. The nondispersive transient photocurrent curves were also obtained for positive carriers in the chiral nematic phase of 3-QTP2MePh-O5* in all the temperature and field ranges as shown in Figure 4, and the carrier mobility was clearly determined for the ranges. The positive carrier mobility was of the order of 10^{-4} cm^2/Vs at 150 °C in the chiral nematic phase; this order of magnitude was identical to that of 3-QTP4-MePhO5* at the same temperature. This value is 1 to 2 orders of magnitude higher than those of conventional nematic liquid crystals with a low

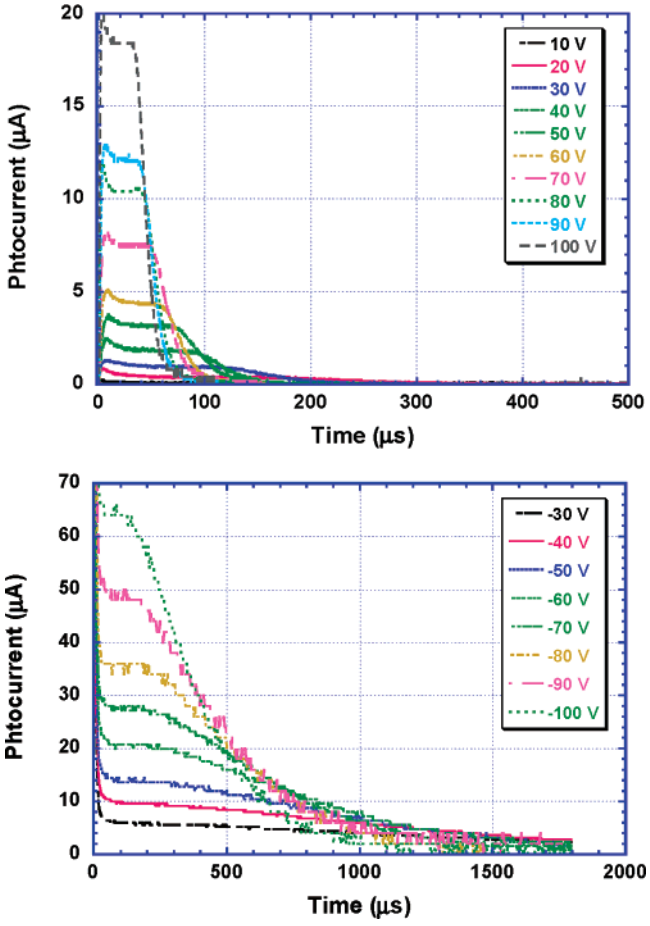

Figure 4. Transient photocurrent curves for (a) positive carriers and (b) negative carriers in the chiral nematic phase of 3-QTP2MePh-O5* at 150 °C. The sample thickness is 9 μm and the wavelength of excitation is 355 nm.

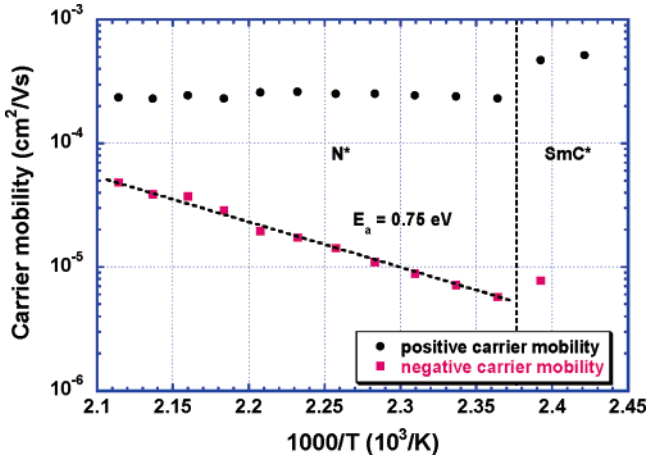

Figure 5. Ahrrenius plot of the carrier mobility in the chiral nematic and isotropic phases of 3-QTP2MePh-O5*.

molecular weight. The positive carrier mobility was almost independent of the electric field; this was different from the case of 3-QTP4MePh-O5* where the positive carrier mobility exhibited the Poole−Frenkel type of dependence. In addition to the field dependence of the positive carrier mobility, its temperature dependence (shown in Figure 5) was quite characteristic: the positive carrier mobility was almost constant in the temperature range in the chiral nematic phase, which was in contrast to the case of 3-QTP4-MePh-O5*.

This behavior did not correspond to that of the viscosity, which strongly depended upon the temperature; the positive carrier transport in the chiral nematic phase of this compound should therefore be attributed to an electronic process. In the isotropic phase, the positive carrier mobility also increased with the temperature. This result indicates that the local molecular assembling structure disappears in the isotropic phase, and the carrier mobility is determined by a thermally activated process without the dynamic disorder effect that causes a negative temperature dependence.

For negative carriers, the nondispersive transient photocurrent curves were obtained in all temperature regions, as shown in Figure 4b; however, in contrast to the positive carrier transport, the negative carrier mobility was about 1 order of magnitude smaller than that of the positive carriers and exhibited the Arrhenius type of temperature dependence. It increased monotonically with the temperature as shown in Figure 5. The activation energy determined from the Arrhenius plot of the negative carrier mobility was 0.7 eV, which was almost identical with that of the viscosity. This result strongly indicates that negative carrier transport in the chiral nematic phase of the compound should be attributed to an ionic process.

The positive carrier mobility increased up to 4×10^{-4} cm^2/Vs from 2×10^{-4} cm^2/Vs discontinuously at the phase transition from the chiral nematic to the chiral smectic C phase; however, the discontinuity was relatively small as compared to that at the transition between the isotropic and smectic phases. In the chiral smectic C phase, only the current decay was observed for the negative carriers and their mobility could not be determined. In the isotropic phase, TOF measurement could not be carried out because the hot stage used for the experiment could not rise the temperature over 200 °C.

Carrier Transport in the Chiral Nematic Phase of 12-QTP2MePh-O5*. This compound had a long alkyl chain and exhibited the chiral nematic phase in a relatively narrow temperature range and the chiral smectic phase in a relatively wide temperature range. In all the temperature regions, the nondispersive transient photocurrent curves were obtained for the positive carriers, and the positive carrier mobility was clearly determined as shown in Figure 6a.

In the chiral nematic phase, the positive carrier mobility was of the order of 10^{-4} cm^2/Vs, which was independent of the electric field and comparable to those in the chiral nematic phase of the other two compounds. However, the temperature dependence of the positive carrier mobility, as shown in Figure 7, was quite peculiar: the positive carrier mobility decreased with an increase in the temperature. At the phase transition temperature from the chiral smectic C to the chiral nematic phase, the mobility was 2×10^{-4} cm^2/Vs, and it decreased to 1×10^{-4} cm^2/Vs at the temperature corresponding to the transition from the chiral nematic to the isotropic phase. The viscosity also decreased monotonically with the temperature in this chiral nematic phase of the compound, and therefore the positive carrier transport should be attributed to the electronic charge carrier transport. In the conventional hopping charge carrier transport, the charge carrier hopping requires thermal activation and

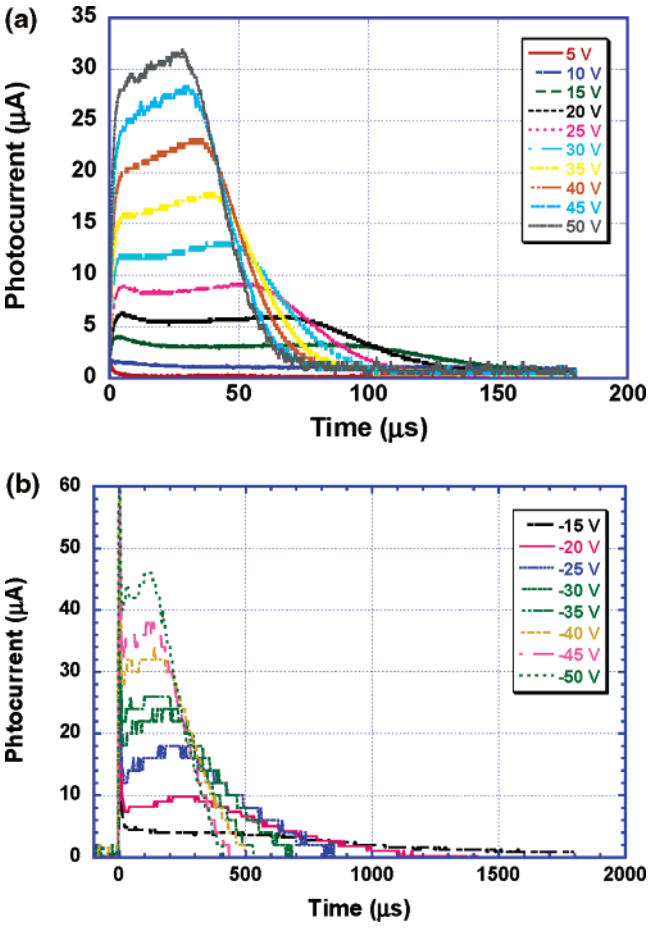

Figure 6. Transient photocurrent curves for (a) positive carriers and (b) negative carriers in the chiral nematic phase of 12-QTP2MePh-O5* at 150 °C. The sample thickness is 9 μm and the wavelength of excitation is 355 nm.

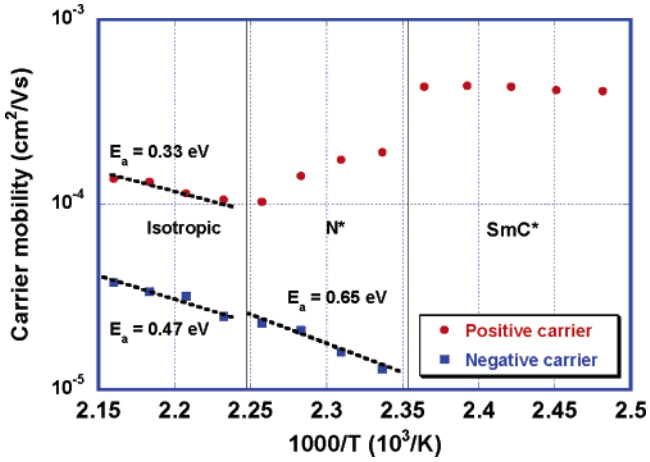

Figure 7. Ahrrenius plot of the carrier mobility in the chiral nematic and isotropic phases of 12-QTP2MePh-O5*.

electric-field assistance, and therefore the carrier mobility increases with the temperature and electric field. In ionic transport, the ionic mobility also increases with the temperature because it is determined by the viscosity of the medium that decreases with an increase in the temperature. In order to explain this negative temperature dependence, a factor (other than these thermally activated processes) that causes a negative temperature dependence must be considered. The positive carrier mobility increased with the temperature in

the isotropic phase, and this can be described by the conventional hopping conduction or ionic transport.

In contrast to the peculiar behavior of the positive carrier transport in the chiral nematic phase, the negative carrier mobility exhibits the Arrhenius type of temperature dependence with an activation energy of 0.5 eV, as shown in Figure 7; this value is identical with that of the viscosity, indicating the ionic nature of the negative charge carrier transport in the chiral nematic phase of the compound. The negative carrier mobility increases continuously with the temperature in the isotropic phase. These characteristics of the negative carrier transport in the chiral nematic and isotropic phases of the compound are identical to those of the other compounds.

In the chiral smectic C phase, the positive carrier mobility was 4×10^{-4} cm^2/Vs, and its dependence on the electric field and temperature was very small. The mobility value was of the same order as in the SmA and SmC phases of 2-phenylnaphthalene and dialkylterthiophene derivatives. The difference in the positive carrier mobility between the chiral nematic and smectic C phases was also small. The small temperature and field dependences of the positive carrier mobility were similar to those in the smectic phases of other liquid-crystalline semiconductors such as 2-phenylnaphthalene and dialkylterthiophene derivatives; this indicates that the positive carrier transport process was intrinsic because the contamination with a fairly small amount of impurity of the order of ppm should change the intrinsic process to an extrinsic trap-controlled hopping process or ionic transport in which the carrier mobility depends upon the temperature,[37] reflecting on trap depth or viscosity.

For the negative carriers, the nondispersive transient photocurrent curves whose kink points appeared in the longer time range were observed in the chiral nematic phase, while only current decays were observed in the chiral smectic C phase. This result indicates that the electron-trapping impurity should play an important roll in the negative carrier transport in the chiral smectic and nematic phases; the impurity functioned as a deep trap for electrons in the chiral smectic phase causing photocurrent decay, and the ionized impurity molecules themselves drifted, thus causing slow ionic conduction in the chiral nematic phase. In the SmX phase which appeared below the SmC* phase, only dispersive transient photocurrent curves both for positive and negative carriers and carrier mobilities could not be determined.

Microscopic Structure of the Chiral Nematic Phases of the Phenylquaterthiophene Derivatives. The nematic phase is an optically uniaxial phase and the chiral nematic phase has a structure in which the uniaxial nematic structure is twisted macroscopically. However, the microscopic aspects of nematic and chiral nematic phases are more complicated. In X-ray diffraction, a weak and broad peak in the low-angle region is frequently observed in nematic and chiral nematic phases. This peak indicates the formation of a microscopic smectic order or clusters, and various researches have suggested a relationship between this smectic order and the anomalous behaviors of viscosity, helical pitch,[38] etc. around the phase transition point from the nematic or chiral nematic phase to the smectic or crystal phase.

The electronic charge carrier transport in organic semiconductors is also strongly affected by the microscopic molecular condensed states. In organic amorphous semiconductors, local energetic and positional disorders strongly influence the microscopic charge carrier hopping and macroscopic carrier transport characteristics. In liquid-crystal systems, the carrier mobility is strongly influenced by the molecular condensed structure in the liquid-crystal phases.[9,13] In this section, we would like to point out that the microscopic smectic order in the chiral nematic phase affects the temperature dependence of the positive carrier mobility.

Figure 8a shows X-ray diffraction patterns in the low-angle region at various temperatures in the chiral nematic phase of 3-QTP4MePh-O5*. In all the temperature regions, a broad halo was observed around $\theta = 20°$, indicating liquid-like short range order and intermolecular spacing in the direction perpendicular to the director. In the low-angle region, no peaks were observed in this phase of the compound in all the temperature regions, indicating no remarkable smectic order or cluster formation even near the crystallization temperature in the chiral nematic phase.

In contrast to 3-QTP4MePh-O5*, a weak but clearly recognizable peak was observed at $2\theta = 2.6°$ in the chiral nematic phase of 12-QTP2MePh-O5* having a long alkyl chain near the phase-transition temperature from the chiral nematic phase to the chiral smectic C phase, as shown in Figures 8, parts b and c. At high temperatures in the phase, this peak was not very remarkable; however, the intensity of the peak increased with a decrease in the temperature and became stronger and sharper below the temperature of the phase transition from the chiral nematic to the chiral smectic phase. The position of the peak corresponded to 34.5 A, which was similar to the magnitude of the molecular length; therefore, this peak should be associated with the cybotactic peak, which indicates a microscopic smectic order or cluster formation.

In the chiral nematic phase of 3-QTP2MePh-O5*, the cybotactic peak was also observed at $2\theta = 3.4°$, which corresponded to 26.0 A; this was identical to the molecular length. However, the cybotactic peak was not as prominent as in the case of 12-QTP2MePh-O5*.

This microscopic smectic order formation reflected in the cybotactic peak in the X-ray diffraction can be explained as a kind of pretransitional effect above the transition temperature of the appearance of the smectic phase.[39] Therefore, a clear cybotactic peak was observed in 12-QTP2MePh-O5* that exhibited the chiral smectic phase in a wide temperature range. A long alkyl chain of the compound should promote the smectic cluster formation in the chiral nematic phase. The small transition enthalpy at the phase transition between the chiral nematic and chiral smectic C phases of 3-QTP2MePhO5* and 12-QTP2MePh-O5* also suggests a microscopic organization in the chiral nematic phases of these compounds.

(37) Funahashi, M.; Hanna, J. *Chem. Phys. Lett.* **2004**, *397*, 319.

(38) Akiyama, H.; Mallia, A.; Tamaoki, N. *Adv. Funct. Mater.* **2006**, *16*, 477.

(39) Chandrasekhar, S. *Liquid Crystals*; Cambridge University Press: Cambridge, 1992.

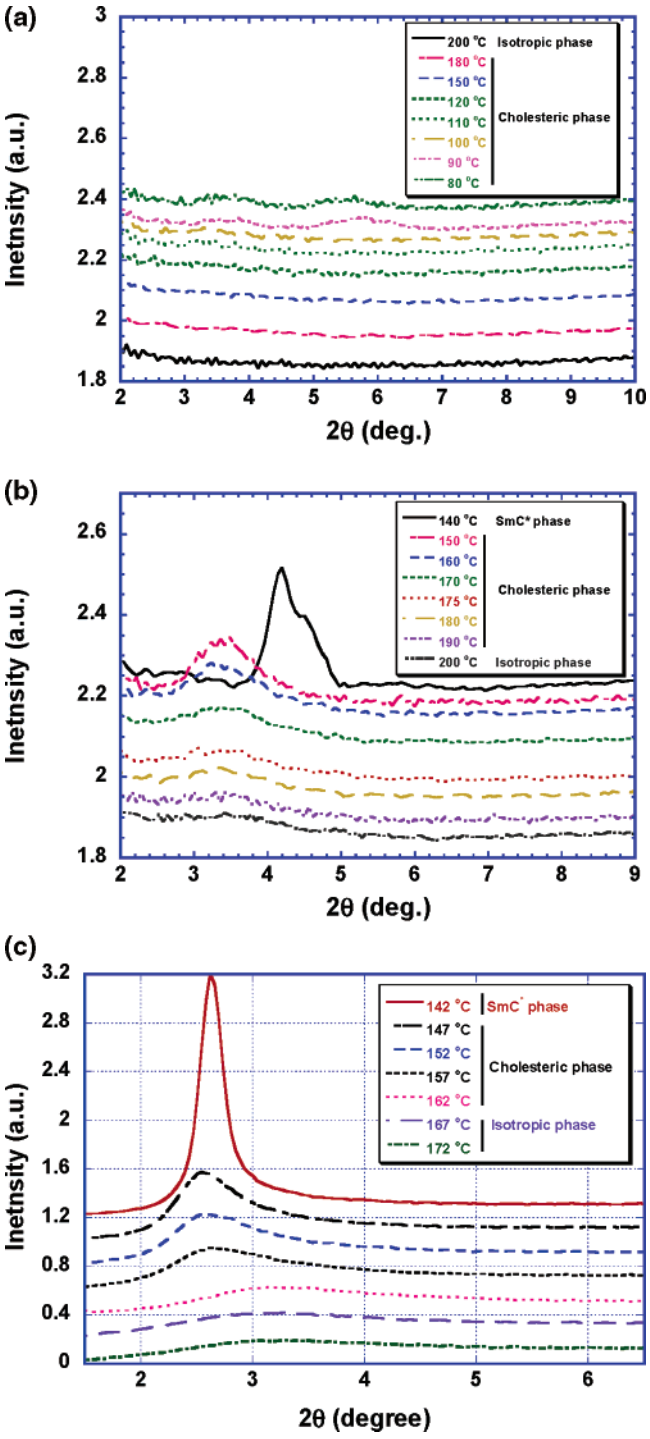

Figure 8. X-ray diffraction curves in the low-angle region. The samples were quartz tubes filled with the liquid crystals without molecular alignment, and the diffraction patterns were measured by an imaging plate. (a) 3-QTP4Me-Ph-O5*. (b) 3-QTP2Me-Ph-O5*. (c) 12-QTP2Me-Ph-O5*.

The temperature dependence of the positive carrier mobility in the chiral nematic phase among the three compounds was quite different. It increased and saturated in the chiral nematic phase of 3-QTP4MePh-O5* with an increase in the temperature, it was independent of temperature in the phase of 3-QTP2MePh-O5*, and it exhibited a negative temperature dependence in the phase of 12-QTP2MePhO5*: This difference in the temperature dependence of the carrier mobility can be explained by the competition between the thermally activated charge carrier hopping causing a positive temperature dependence and the pretransitional microscopic smectic order formation, which is suggested by the cybotactic peak in the X-ray diffraction pattern and degraded by the dynamic disorder effect, resulting in a negative temperature dependence of the carrier mobility. In the chiral nematic phase of 3-QTP4MePh-O5*, no remarkable pretransitional molecular organization was observed, and therefore the carrier mobility decreased with a decrease in the temperature because of thermally activated charge carrier hopping. In contrast, the carrier mobility did not decrease with a decrease in the temperature in the chiral nematic phase of 3-QTP-2MePh-O5* because the pretransitional microscopic smectic order formation promoted the intermolecular hopping of charge carriers. In the chiral nematic phase of 12-QTP2MePh-O5* in which this effect was very prominent, the decrease in the charge carrier hopping rate caused by a decrease in the temperature should be canceled and exceeded by the promotion of charge carrier hopping by the pretransitional microscopic order formation, resulting in a negative temperature dependence of the carrier mobility.

The small differences in the positive carrier mobility between the chiral nematic and smectic C phases of 3-QTP2MePh-O5* and 12-QTP2MePh-O5* should also be explained by this pretransitional microscopic organization. The differences were only a factor of 2 in these two compounds, which was much smaller than those between the isotropic and smectic A or smectic C phases of 2-phenylnaphthalene and dialkylterthiophene in spite of the liquid-like nature of the chiral nematic phases.[9,13] The smectic order formation in the chiral nematic phases should enhance the positive carrier mobility in addition to the realization of electronic carrier transport.

In contrast to the variety in the temperature dependence of the positive carrier mobility, the temperature dependences of the negative carrier mobility of the chiral nematic phases of the three compounds were quite similar. They were of the Arrhenius type, and the activation energies were identical to those of the viscosities. It is plausible that the impurity molecules that trapped electrons were contaminated in these three compounds, and they trapped electrons and formed a negatively charged ionic species that drifted in the bulk, thus causing ionic conduction in the chiral nematic phases of these compounds. The synthesis and purification procedures were common among the three compounds, and it is reasonable to assume that these three compounds contained the same type of impurities.

The smectic-like order formation in the chiral nematic phase should affect not only the electronic transport but also the viscosity and ionic carrier transport. In the chiral nematic phases of 3-QTP2MePh-O5* and 12-QTP2MePh-O5* in which the pretransitional smectic order formation is remarkable, the activation energies of the viscosity and negative carrier mobility are 0.6 and 0.7 eV, respectively; these values are larger than those of the chiral nematic phase of 3-QTP4MePh-O5* with no remarkable pretransitional order formation. The larger activation energy should be attributed to the pretransitional smectic order formation.

In the recent report by M. O'Neil et al.,[25] high carrier mobilities on the order of 10^{-4} cm^2/Vs with small temper-

ature-dependence were observed in the nematic phases of dialkylfluorene derivatives with large π-conjugated system and short lateral alkyl chains while low carrier mobilities which was dependent on temperature were observed in the nematic phases of those with relatively small π-conjugated system and long lateral alkyl chains. Large π-conjugated systems increased intermolecular transfer integral to enhance intermolecular charge carrier transfer, and on the other hand, long lateral alkyl chains inhibit close molecular packing to decrease intermolecular charge transfer. Large transfer integrals contribute to a small activation energy of intermolecular charge carrier hopping and should increase carrier mobility, decreasing its temperature-dependence. In X-ray diffraction in the nematic phases of the liquid crystals with high carrier mobility, no cybotactic peak associated with microscopic smectic order was observed, but a weak diffraction was observed in a low angle region which was related to short range order in the lateral direction. Microscopic structure in the chiral nematic phases of our phenylquaterthiophene derivatives should be different from the nematic phases of those dialkylfluorene derivatives because of the relatively long alkyl chains at the lateral position of fluorene ring.

In summary, the carrier transport characteristics in the chiral nematic phases of three phenylquaterthiophene derivatives were investigated using the time-of-flight technique. The temperature dependences of the negative charge carrier mobility in the chiral nematic phases of these compounds were of the Arrhenius type, and the activation energies corresponded to those of the viscosity of the phases. Therefore, the negative carrier transport should be attributed to the ionic transport, and the negative ionic carriers should be ionized impurity molecules. In contrast to the ionic nature of the negative carrier transport, the positive carrier transport in the chiral nematic phases of the compounds should be attributed to the electronic charge carrier transport. The temperature dependence of the positive carriers in the chiral nematic phases of the compounds was strongly affected by the pretransitional effect. A negative temperature dependence was observed in the chiral nematic phase of 12-QTP2MePh-O5*, and a temperature-independent mobility was observed in the chiral nematic phase of 3-QTP2MePh-O5*, where a smectic-like order was formed; positive temperature dependence was observed in the phase of 3-QTP4MePh-O5*, where no pretransitional organization was observed. Such a smectic-like order formation occurred in the chiral nematic phase below the temperature at which the SmC* phase appeared.

Acknowledgment. We thank the Association for the Progress of New Chemistry, Sumitomo Foundation, and Grants-in-Aid for Scientific Research (No. 16750185) from the Ministry of Education, Culture, Sports, Science and Technology for financial support.

CM0621287